PROCESSING ROUTES FOR THE PREPARATION OF POLYLACTIC-ACID/CELLULOSE-NANOWHISKER NANOCOMPOSITES FOR PACKAGING APPLICATIONS

Leandro N. Ludueña[1], Juan I. Moran[2], Thanh Vu Phuong[3], Patrizia Cinelli[4], Andrea Lazzeri[5], Vera A. Alvarez[6]

[1,2,6] Composite Materials Group (CoMP) – National Research Institute of Materials Science and Technology (INTEMA) - National Research Council (CONICET) - National University of Mar del Plata (UNMdP), Mar del Plata, Argentina.
[3,4,5] Industrial Chemistry and Material, Department of Chemical Engineering Science, University of Pisa, Pisa, Italy.

Abstract
In this work polylactic-acid (PLA)/cellulose-nanowhisker (CNW) nanocomposites were prepared by twin screw extrusion followed by injection molding. The CNW was dispersed in a plasticizer/compatibilizer (PL) previous to the melt mixing process. It was found that the PL not only improved the procesability and reduced the fragility of PLA but also prevented the agglomeration of the CNW up to 12 wt.% of CNW content, obtaining well dispersed and distributed PLA/CNW nanocomposites. The prepared nanocomposites were injection molded and their mechanical/thermal properties were evaluated. PLA/CNW nanocomposites showed higher mechanical properties than those of the neat matrix but the material with the lower CNW content showed the best mechanical performance.

1. Introduction
The development of environmental-friendly biodegradable polymeric materials from renewable sources has attracted extensive interest [1-2]. This is mainly due to the waste accumulation and also the ever-increasing oil price, which are currently a serious concern. PLA is biodegradable, thermoplastic, aliphatic polyester derived from renewable resources such as starch and appears as one of the best sustainable alternative to petrochemical-derived products [3]. PLA has been found to have good stiffness and strength, it can be processed with conventional plastic processing machinery (extrusion, blow molding, injection molding, vacuum forming) and is being used in several applications, such as food packaging, water and milk bottles, degradable plastic bags as well as in automotive applications [4]. Products made from PLA are biodegradable and are found to fully disappear in less than 30 days in ideal conditions [5-6]. The performance of PLA can be greatly enhanced by the addition of nano-reinforcements. Natural fibers have many advantages compared to synthetic fibers, low weight, reduced tool wearing and they are also recyclable and biodegradable [7]. Moreover, in order to develop a fully eco-friendly polymer nanocomposite, the use of a reinforcement derived from renewable biomass is needed. Cellulose is the main component of several natural fibers and agricultural byproducts [8]. The structure of the natural fiber consist on cellulose, which awards the mechanical properties of the complete fiber, ordered in microfibers enclosed by the other two main components: hemicellulose and lignin [9]. Cellulose microfibers can be found as intertwined microfibers in the cell wall (2-20 μm diameter and 100-40,000 nm long depending on its source) [10]. It is a linear polymer of β-(1⟶4)-D-glucopyranose units. The mechanical properties of cellulose microfibers depend on the cellulose polymorph present, which are named cellulose I, II, III and IV; being type I the one showing better mechanical properties. Hemicellulose is composed of different types of cycled saccharides such as xylose, mannose and glucose, among others. It forms a highly branched random structure and it is mainly amorphous [11]. Lignins are amorphous polymers formed by phenyl-propane units. They mainly consist of aromatic units such as guaiacyl, syringyl and phenylpropane [8]. As well as these microfibers, there

are cellulose nanowhiskers (CNW) conformed by nanocrystalline domains and amorphous regions [10]. A controlled acid hydrolysis can separate both regions driving to crystalline domains with an elastic modulus of 150 GPa, which is higher than that of the S-glass (85 GPa) and Aramid fibers (65 GPa). Because of the good mechanical properties, the production CNW has generated a great interest. In the last years these fibers also attracted much attention due to environmental concerns especially for the reinforcement of biodegradable polymers to produce fully biodegradable micro/nanocomposites with enhanced mechanical properties [12-19]. One challenge when using these fibers is that, due to their polar surfaces, it is difficult to disperse them uniformly in a non-polar medium. This might be the reason why the processing of cellulose nanocomposites was first limited to solvent casting, where water soluble polymers were the most common matrices [20]. However, the development of other, more flexible and industrially viable processing techniques is necessary in order to promote commercialization of these materials. One of the developed processing methods has been melt compounding. The melt compounding of CNW nanocomposites presents several challenges. The major difficulties are to feed the CNW into the extruder and achieve uniform dispersion in the non-polar polymer matrix. The CNW have a very high surface area and have a tendency to aggregate when dried [21]. This problem can be overcome by dispersing the CNW in a suitable medium which is then fed into the extruder, or first dried and then extruded [22].
The aim of this work was to prepare PLA/CNW nanocomposites by melt blending. We proposed a processing route to achieve good dispersion and distribution of the fibers inside the matrix by selecting/changing/optimizing the processing parameters. The final morphology of the nanocomposites was analyzed by scanning electron microscopy (SEM) and mechanical/thermal properties were studied by means of tensile tests and differential scanning calorimetry, respectively.

2. Experimental

Materials

Polylactic acid (PLA 3051D) in pellet form was obtained from Nature Works. It has a specific gravity of 1.24 g/cm3 and a melt flow index of 14 g/10 min (2100C/ 2.16 kg). Cellulose nanowhisker slurry named Celish (Celish KY110G water slurry containing 10 wt.% CNW, purchased from Daicel Chemical Industries, Ltd., Japan) was used as filler. The plasticizer (PL) used to facilitate the melt processing and to reduce the fragility of PLA is being patented, therefore its formulation will not be revealed in this work.

Preparation of nanocomposites

A mixture of 30 g of Celish, 27 g. of PL and 50ml. of water was continuously stirred at room temperature for 15min. The water was added to decrease the viscosity of the solution for easier stirring. The mixture was dried in an oven at 110 ºC for 2 h. Under these drying conditions only water is evaporated from the solution and the PL should act preventing the agglomeration of the CNW. The final slurry was named CNWPL1 which consisted on 10 wt.% of CNW and 90 wt.% of PL. Same procedure but using different Celish, PL and water contents was followed to prepare a slurry with 40 wt.% of CNW and 60wt.% of PL named CNWPL2. Nanocomposites with 82/18/0, 80/18/2 and 70/18/12 PLA/PL/CNW wt.% ratios were prepared by the melt blending of 8.2 gr. of PLA with 1.8 g of PL; 8gr. of PLA with 2 g of CNWPL1 and 7 g of PLA with 3 g of CNWPL2, respectively, in a twin screw extruder Thermo Scientific Haake Minilab II. Temperature, screw speed and residence time were set at 190 ºC, 90 rpm and 1 min, respectively. Table 1 shows the nomenclature and composition of the different samples.

Table 1. Composition of the different injection molded samples.

Material	PLA (wt.%)	CNW (wt.%)	PL (wt.%)
PLA18	82	0	18
2PLA18	80	2	18
12PLA18	70	12	18

Finally, bone shaped samples (Fig. 1a) were injection molded at a melt temperature and mold temperature of 190 ºC and 38 ºC, respectively. The injection molding parameters are shown in Fig. 1b.

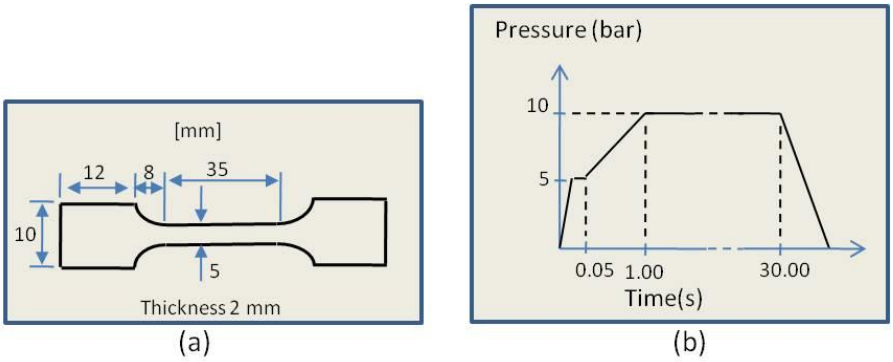

Figure 1. Injection molding: (a) dimensions of the samples, (b) injection parameters.

Methods

The content of CNW in the Celish slurry was calculated by drying the slurry at 110 ºC in vacuum oven until constant weight.

Thermogravimetrical Analysis (TGA) was carried out in a TA Instruments TGA Q500 from 30 °C to 600 °C at 10 °C/min under nitrogen atmosphere. Derivative Thermogravimetrical Analysis (DTGA) was performed from the derivative of the residual mass as a function of temperature. The temperature for the onset of thermal degradation (T_{on}) was calculated from TGA curves at 5% mass loss. The temperature for the maximum thermal degradation rate (T_{max}) was calculated from the main peak of DTGA curves.

Differential Scanning Calorimetry (DSC) measurements were performed in a TA Instruments model Q2000 calorimeter, operating from 25 to 200ºC at a heating rate of 5ºC/min under nitrogen atmosphere. The glass transition temperature (T_g), cold crystallization temperature (T_c), pre-melt crystallization temperature (T_{pc}), melting temperature (T_m) and heat of melting (ΔH_m) were determined for the different materials. Details of cold crystallization and pre-melt crystallization for PLA can be found in the literature [23]. The degree of crystallinity (X_{cr}) of each sample was calculated from the following equation:

$$X_{cr}(\%) = \frac{\Delta H_m}{w_{PLA} \times \Delta H_{100}} \times 100 \qquad (1)$$

where ΔH_m is the experimental heat of melting, w_{PLA} the PLA weight fraction and ΔH_{100} is the heat of melting of 100 % crystalline PLA and its value is 93 J/g [24]. To determine the crystallinity of the sample, the heats of cold crystallization and pre-melt crystallization were subtracted from heat of melting [23]. The resulting value was called ΔH_m.

The morphology of the fibers inside the nanocomposites was analyzed by SEM. A Jeol JSM-5600LV Scanning Electron Microscopy was used. Micrographs of the cryo-fractured surfaces of the samples were taken.

Mechanical properties were analyzed in a universal testing machine INSTRON 4467 at a crosshead speed of 3 mm/min at 25 ºC and 74% RH. The injection molded specimens were used for tensile testing and the gauge length was 30 mm. The Young´s modulus (E) was calculated from the initial part of the slope of the stress–strain curves. Maximum tensile stress (σ) and elongation at break (ε) were also reported. At least five test samples were tested for each material and the average values are presented.

3. Results and Discussion

Figure 2 shows the results of the thermogravimetrical analysis for the neat matrix and nanocomposites. Table 2 shows the temperatures for the onset of thermal degradation (T_{on}) and the maximum thermal degradation rate (T_{max}).

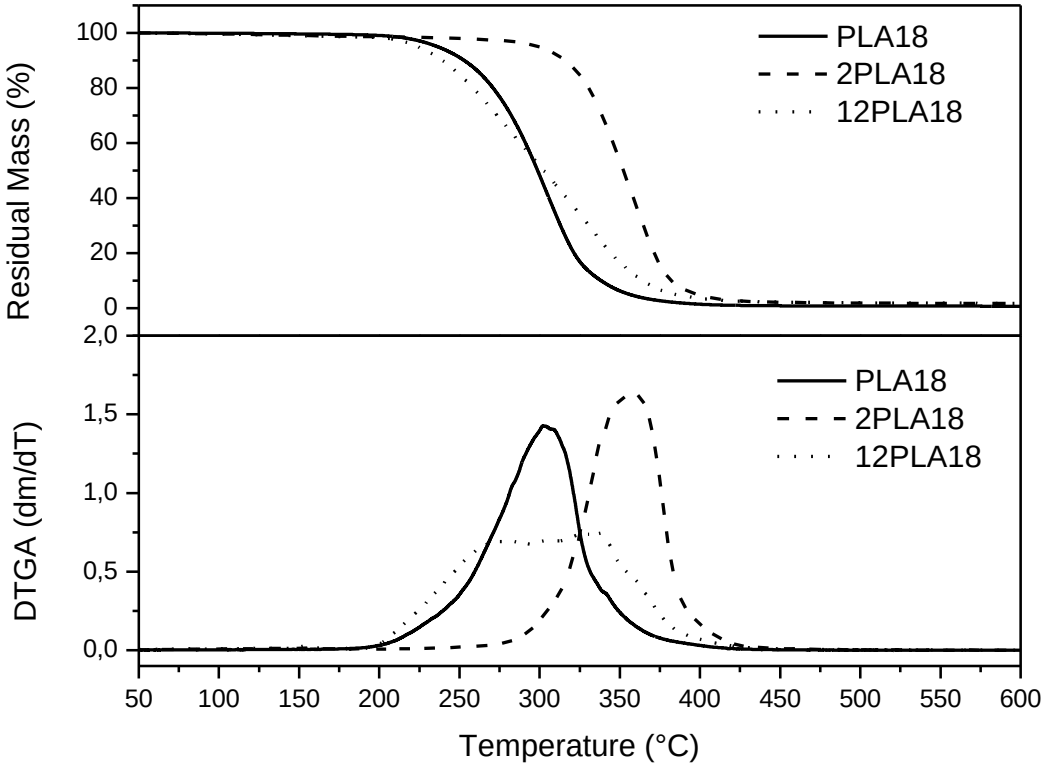

Figure 2. Thermogravimetrical analysis for the neat matrix and nanocomposites.

The addition of 2wt.% CNW significantly improved the thermal stability of PLA18. The onset of the PLA18 degradation process shifted from 236°C to 300°C. T_{max} was also shifted from 302°C to 359°C. The nanocomposite with 12wt.% of CNW shows two stage thermal degradation process. The first peak at T_{max} 282°C is associated with the thermal degradation of CNW. This value is in the range of previous results for CNW obtained from different sources [19]. In the case of 2PLA18 only one stage is observed, probably because the CNW content is not high enough to produce such a peak and is remains masked by the PLA18 thermal degradation process. The results showed that all materials were thermally stable in the region below 224°C. Then, the recommended processing

temperature of these materials is 224°C. Both PLA18 and nanocomposites could maintain more than 95% of their original weight at this temperature.
Figure 3 shows the DSC thermograms displaying the heating ramp including T_g, T_{cc}, T_{pc} and T_m for all materials. Similar curves were observed by Ljungberg [23] for plasticized PLA films,

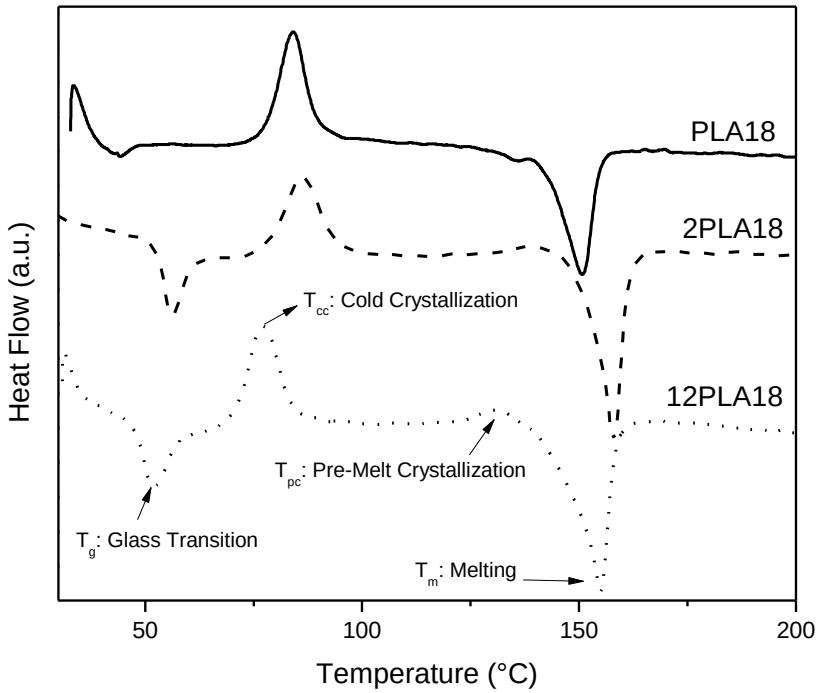

Figure 3. DSC curves for the neat matrix and nanocomposites.

The thermal characteristics T_g, T_{cc}, T_{pc}, T_m, ΔH_m, and X_{cr} obtained from DSC are reported in Table 2.

Table 2. Thermal properties of PLA and PLA/CNW nanocomposites

Material	TGA Parameters		DSC Parameters					
	T_{on} (°C)	T_{max} (°C)	T_g (°C)	T_{cc} (°C)	T_{pc} (°C)	T_m (°C)	ΔH_m (J/gr)	X_{cr} (%)
PLA18	236	302	44.2	84.3	138.9	150.8	2.6	2.8
2PLA18	300	359	57.5	89.6	139.5	155.7	5.9	6.5
12PLA18	224	282 – 339	54.0	81.1	134.0	154.4	11.2	13.6

It can be seen that T_g increase with the addition of fiber to the PLA. T_g can increase or decrease with the degree of crystallinity depending on the relative density of the amorphous and crystalline states. Most often the more orderly crystalline state has the higher density at T_g and the non-crystalline molecular chains are constrained by being anchored to the immobile crystallites and T_g increases. On rare occasions the crystalline state has a lower density than the amorphous material. In this case, less constraint on the non-crystalline chain segments increases the entropy causing T_g to decrease [23]. The increment of T_g is supported by the increment of the crystallinity degree of the

PLA18 with the addition of the fiber (Table 2). This can be explained by the nucleating ability of CNW allowing the crystallization of PLA [7].

T_{cc}, T_{pc} and T_m increase with the addition of 2wt.% of CNW to the PLA18. These parameters decreased adding 12wt.% of CNW. The T_{cc} and T_{pc} values of 12PLA18 were even lower than that of the PLA18. This is a consequence of a balance between nucleation ability of CNW and the reduced mobility of polymer chains in the presence of rigid CNW fibers. Regarding polymer/natural-fiber nanocomposites, heterogeneous nucleation on the fiber surfaces may be the main mechanism responsible of the crystallization behavior of the matrix. In such case, a high density of nuclei along the interface hinder the lateral extension and force spherulities to growth in one direction, perpendicularly to the filler surfaces, and result in a columnar layer, known as transcrystalline layers; but depending on the filler nature and content, transcrystallization may be restricted by filler–filler contacts and agglomeration which reduce the filler exposed surface area [25-27].
Figure 4 shows the SEM micrographs of the cryo-fractured surface of the samples.

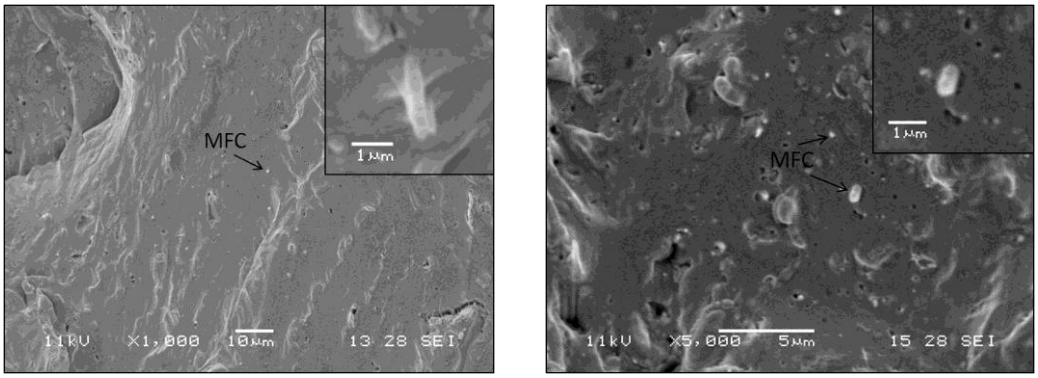

(a) **(b)**

Figure 4. SEM micrographs of the cryo-fractured surface of: (a) 2PLA18; (b) 12PLA18.

It can be seen that the CNW (white points indicated by black arrows) are well distributed and dispersed in both 2PLA18 and 12PLA18 nanocomposites. The magnifications in the upper-right corner of the micrographs show that the diameter of the dispersed CNW is about 100 nm. This result demonstrates that the plasticizer acts as dispersion agent preventing the agglomeration of CNW during the water evaporation process of the CNWPL1 and CNWPL2 slurries. It must be also taken into account that the main function of the plasticizer is to improve the performance of PLA when it is processed by melt blending. Iwatake et al. [3] compared the morphology of PLA/CNW nanocomposites prepared by two techniques, solvent mixing method and direct melt mixing. The solvent method consisted on mixing Celish slurry, acetone and PLA together, evaporating the water and acetone in vacuum oven and then kneading the PLA/CNW free solvent mixture in a twin rotary roller mixer. The direct melt mixing method was carried out by the addition of the Celish slurry into the twin rotary roller mixer after melting PLA18. The first method has the advantage of using a dispersion agent to prevent CNW agglomeration while the second one is industrially applicable. They found well distributed and dispersed CNW in the PLA/CNW nanocomposites prepared by the solvent method while many agglomerations were observed in the nanocomposite made by the direct mixing method [3]. The method proposed in our work can be thought as a mixture of the processes before mentioned making use of the advantages (dispersion agent for CNW, industrial scale) while avoiding the disadvantages (poor dispersion of CNW, laboratory scale) of them.
Table 3 shows the mechanical properties of the matrix and their nanocomposites.

Table 3. Mechanical properties of PLA and PLA/CNW nanocomposites

Material	E (GPa)	σ (MPa)	ε (%)
PLA18	1.25 ± 0.25	27 ± 4	55 ± 3
2PLA18	1.99 ± 0.64	35 ± 3	43 ± 2
12PLA18	1.75 ± 0.23	29 ± 2	40 ± 6

The Young´s moduli and strength of the nanocomposites were higher than that of the neat matrix because of the reinforcing effect of the CNW. On the other hand, the elongation at break was lower for the nanocomposites due to the presence of the fibers that may be immobilizing the polymer chains decreasing the polymer ductility. Contrarily to the expected results, the nanocomposite with the lower CNW content showed the highest mechanical properties. This result can be attributed to the agglomeration of the CNW filler but, as was previously mentioned, it could not be demonstrated by SEM since the same dispersion and distribution of the CNW reinforcement in both nanocomposites was observed. Our hypothesis is that the higher PL content of the CNWPL2 slurry could be changing the chemical structure of the CNW. Therefore, in future works the morphology, the chemical structure and the thermal stability of the CNW as a function of the PL wt.% will be analyzed.

Conclusions

In this work polylactic-acid/cellulose-nanowhisker nanocomposites were prepared by twin screw extrusion. The plasticizer used to facilitate the melt processing and to reduce the fragility of PLA also prevented the agglomeration of the CNW at least up to 12 wt.% of filler, obtaining well dispersed and distributed PLA/CNW nanocomposites. The mechanical properties of the nanocomposites were higher than that of the neat matrix but the nanocomposite with the lower CNW content showed the best mechanical performance which could be attributed to changes in the CNW chemical structure.

Acknowledgements

Authors acknowledge to ANPCyT, MINCyT (Fonarsec FSNano004), UNMdP, CONICET (Argentine) and CNR (Italy) for the financial support.

References

1. Bénédicte Lepoittevin, Myriam Devalckenaere, Nadège Pantoustier, Michaël Alexandre, Dana Kubies, Cédric Calberg, Robert Jérôme, Philippe Dubois. *Poly([var epsilon]-caprolactone)/clay nanocomposites prepared by melt intercalation: mechanical, thermal and rheological properties.* Polymer, 2002. **43**(14): p. 4017-4023.
2. Bhardwaj, R. and A.K. Mohanty. *Modification of Brittle Polylactide by Novel Hyperbranched Polymer-Based Nanostructures.* Biomacromolecules, 2007. **8**(8): p. 2476-2484.
3. Iwatake, A., M. Nogi, and H. Yano. *Cellulose nanofiber-reinforced polylactic acid.* Composites Science and Technology, 2008. **68**(9): p. 2103-2106.
4. Antonio Norio Nakagaito, Akihiro Fujimura, Toshiaki Sakai, Yoshiaki Hama, Hiroyuki Yano. *Production of microfibrillated cellulose (MFC)-reinforced polylactic acid (PLA) nanocomposites from sheets obtained by a papermaking-like process.* Composites Science and Technology, 2009. **69**(7–8): p. 1293-1297.
5. Oksman, K., M. Skrifvars, and J.F. Selin. *Natural fibres as reinforcement in polylactic acid (PLA) composites.* Composites Science and Technology, 2003. **63**(9): p. 1317-1324.

6. Mathew, A.P., K. Oksman, and M. Sain. *Mechanical properties of biodegradable composites from poly lactic acid (PLA) and microcrystalline cellulose (MCC).* Journal of Applied Polymer Science, 2005. **97**(5): p. 2014-2025.
7. Ludueña, L., A. Vázquez, and V. Alvarez. *Effect of lignocellulosic filler type and content on the behavior of polycaprolactone based eco-composites for packaging applications.* Carbohydrate Polymers, 2012. **87**(1): p. 411-421.
8. Baillie, C.. *Green composites: polymer composites and the environment*, in *Abington Hall, Abington Cambridge CB1 6AH, England*, D.T. Nishino, Editor. 2004, Woodhead Publishing Limited: Department of Chemical Science and Engineering, Faculty of Engineering, Kobe University. p. 49-80.
9. Placet, V.. *Characterization of the thermo-mechanical behaviour of Hemp fibres intended for the manufacturing of high performance composites.* Composites Part A: Applied Science and Manufacturing, 2009. **40**(8): p. 1111-1118.
10. Itoh, T. and R.M. Brown. *The assembly of cellulose microfibrils in <i>Valonia macrophysa</i> Kütz.* Planta, 1984. **160**(4): p. 372-381.
11. Xiao, B., X.F. Sun, and R. Sun. *Chemical, structural, and thermal characterizations of alkali-soluble lignins and hemicelluloses, and cellulose from maize stems, rye straw, and rice straw.* Polymer Degradation and Stability, 2001. **74**(2): p. 307-319.
12. Morin, A. and A. Dufresne. *Nanocomposites of Chitin Whiskers from Riftia Tubes and Poly(caprolactone).* Macromolecules, 2002. **35**(6): p. 2190-2199.
13. Petersson, L., I. Kvien, and K. Oksman. *Structure and thermal properties of poly(lactic acid)/cellulose whiskers nanocomposite materials.* Composites Science and Technology, 2007. **67**(11-12): p. 2535-2544.
14. Dufresne, A., D. Dupeyre, and M.R. Vignon. *Cellulose microfibrils from potato tuber cells: Processing and characterization of starch-cellulose microfibril composites.* Journal of Applied Polymer Science, 2000. **76**(14): p. 2080-2092.
15. Azizi Samir, M.A.S., F. Alloin, and A. Dufresne. *Review of Recent Research into Cellulosic Whiskers, Their Properties and Their Application in Nanocomposite Field.* Biomacromolecules, 2005. **6**(2): p. 612-626.
16. Hanna Lönnberg, Linda Fogelström, My Ahmed Said Azizi Samir, Lars Berglund, Eva Malmström, Anders Hult. *Surface grafting of microfibrillated cellulose with poly([epsilon]-caprolactone) - Synthesis and characterization.* European Polymer Journal, 2008. **44**(9): p. 2991-2997.
17. William J. Orts, Justin Shey, Syed H. Imam, Gregory M. Glenn, Mara E. Guttman, Jean-Francois Revol. *Application of Cellulose Microfibrils in Polymer Nanocomposites.* Journal of Polymers and the Environment, 2005. **13**(4): p. 301-306.
18. Lagaron, J.M. and A. Lopez-Rubio. *Nanotechnology for bioplastics: opportunities, challenges and strategies.* Trends in Food Science & Technology. **In Press, Corrected Proof**.
19. Leandro N. Ludueña, Antonella Vecchio, Pablo M. Stefani and Vera A. Alvarez. *Extraction of Cellulose Nanowhiskers from Natural Fibers and Agricultural Byproducts.* Fibers and Polymers, 2013. **14**(7): p. 1118-1127.
20. Petersson, L., I. Kvien, and K. Oksman. *Structure and thermal properties of poly(lactic acid)/cellulose whiskers nanocomposite materials.* Composites Science and Technology, 2007. **67**(11–12): p. 2535-2544.
21. Daniel Pasquini, Eliangela de Morais Teixeira, Antonio Aprigio da Silva Curvelo, Mohamed Naceur Belgacem, Alain Dufresne. *Surface esterification of cellulose fibres: Processing and characterisation of low-density polyethylene/cellulose fibres composites.* Composites Science and Technology, 2008. **68**(1): p. 193-201.

22. K. Oksman, A.P. Mathew, D. Bondeson, I. Kvien. *Manufacturing process of cellulose whiskers/polylactic acid nanocomposites.* Composites Science and Technology, 2006. **66**(15): p. 2776-2784.
23. Ljungberg, N. and B. Wesslén. *Preparation and Properties of Plasticized Poly(lactic acid) Films.* Biomacromolecules, 2005. **6**(3): p. 1789-1796.
24. Vasanthakumari R, Pennings A. Crystallization kinetics of poly(l-lactic acid). Polymer, 1983. **24**(2): p. 175-178.
25. Cai, Y., Petermann, J. and Wittich, H. Transcrystallization in fiber-reinforced isotactic polypropylene composites in a temperature gradient. Journal of Applied Polymer Science, 1997. **65**(1): p. 67–75.
26. Quan, H., Li, Z.-M., Yang, M.-B. and Huang, R. On transcrystallinity in semicrystalline polymer composites. Composites Science and Technology, 2005. **65**(7–8): p. 999–1021.
27. Son, S.-J., Lee, Y.-M. and Im, S.-S. Transcrystalline morphology and mechanical properties in polypropylene composites containing cellulose treated with sodium hydroxide and cellulase. Journal of Materials Science, 2000. **35**(22): p. 5767–5778.